Anal. Chem. **2005,** *77,* 4792−4799

Detection of a Chemical Warfare Agent Simulant in Various Aerosol Matrixes by Ion Mobility Time-of-Flight Mass Spectrometry

Wes E. Steiner, Steve J. Klopsch, William A. English, Brian H. Clowers, and Herbert H. Hill*

Department of Chemistry, Washington State University, Pullman, Washington 99164-4630

For the first time, a traditional radioactive nickel (^{63}Ni) β emission ionization source for ion mobility spectrometry was employed with an atmospheric pressure ion mobility orthogonal reflector time-of-flight mass spectrometer (IM-(tof)MS) to detect a chemical warfare agent (CWA) simulant from aerosol samples. Aerosol-phase sampling employed a quartz cyclonic chamber for sample introduction. The simulant reference material, which closely mimicked the characteristic chemical structure of CWAs as defined and described by Schedule 1, 2, or 3 of the Chemical Warfare Convention treaty verification, was used in this study. An overall elevation in arbitrary signal intensity of ~1.0 orders of magnitude was obtained by the progressive increase of the thermal AP-IMS temperature from 75 to 275 °C. A mixture of one G-type nerve simulant (dimethyl methylphosphonate (DMMP)) in four (water, kerosene, gasoline, diesel) matrixes was found in each case (AP-IMS temperature 75−275 °C) to be clearly resolved in less than 2.20×10^4 μs using the IM(tof)MS instrument. Corresponding ions, masses, drift times, K_o values, and arbitrary signal intensities for each of the sample matrixes are reported for the CWA simulant DMMP.

International implementation of the Chemical Weapons Convention (CWC) treaty, which banned the development, production, acquisition, retention, and direct or indirect transfer of chemical weapons, mandated destruction of all chemical weapons held in reserve.[1] These requirements lead to improvements in analytical technology[2] to not only detect trace amounts of particularly acutely toxic chemicals, such as chemical warfare agents (CWA), but for the safe handling and verification of CWAs and weapons containing CWAs (bombs, rockets, mines, other munitions) being transported to disposal facilities for destruction (typically incineration methods).[3] Complicating the issue, however, is the actual transportation of these CWA-related materials and the elevated risks they potentially possess for accidental exposure, particularly in densely populated areas. In light of this, improvements in analytical technology in recent years, especially since the events of September 11, 2001, has now shifted focus from the development of analytical methods for verification to methods of rapid detection and alarm for homeland security. Thus, it is imperative to continue the research and development of analytical technology to help ensure that future aqueous and gaseous resources relied upon by civilian populations[4] are not compromised.

Under standard atmospheric conditions (e.g., 25 °C, 760 Torr), CWAs are reactive and possess varying degrees of environmental lifetimes depending upon their method of dissemination.[5] One of the major threats presented by a CWA release, or munitions containing a CWA exploding overhead, is that of an airborne dispersal of a liquefied CWA matrix resulting in extremely hazardous contaminant aerosols of various sizes. The larger contaminant aerosol droplets would have a propensity to deposit near the point of release, causing in some cases a significant amount of ground or contact surface contamination. Smaller droplets would be likely to remain suspended as an aerosol, forming a primary cloud, which may under certain environmental conditions (i.e., temperature, pressure, wind speed, terrain profile, etc.) be transported through the atmosphere over substantial distances. Vaporization of deposited contaminant liquid on the ground or contact surfaces forms a secondary cloud. For the more persistent (i.e., low vapor pressure) CWAs, substantial ground or contact surfaces contamination can be found to have extended lifetimes; while most of the more volatile CWA s are contained in the secondary cloud.[6] Although rapid detection methods for CWA gases from secondary clouds have been developed for some time, the detection of CWAs within a primary aerosol cloud may prove difficult depending upon the aerosol's nature and matrix.

Chemical warfare agents have been classified historically as nerve, vesicant, or blood borne agents. The nerve agents—sarin (GB), soman (GD), tabun (GA), and VX—all disrupt neurological regulation within biological systems through the inhibition of acetyl cholinesterase.[7] The vesicant agents (also known as bifunction alkylating agents) sulfur mustard gas (HD), lewisite (L), nitrogen mustard gas (HN), and phosgene-oxime (CX) are

* To whom correspondence should be addressed. Tel: (509) 335-5648. Fax: (509) 335-8867. E-mail: hhhill@wsu.edu.

(1) *Chemical Weapons Convention (CWC) bans the development, production, acquisition, stockpiling, and use of Chemical Weapons and on there destruction.* Washington D. C. United States Bureau of Arms Control and Disarmament Agency, Entered into force April 29, 1997.

(2) Hill, H. H.; Martin, S. *Pure Appl. Chem.* **2002**, *74*, 2281−2291.

(3) Yang, Y. C. *Chem. Ind.* **1995**, *9*, 334. Yang, Y. C.; Baker, J. A.; Ward, J. R. *Chem. Rev.* **1992**, *92*, 1729. Lion, C.; Da Conceicao, L.; Magnaud, G.; Delmas, G.; Desgranges, M. *Rev. Sci. Tech. Def.* **2001**, *52*, 139.

(4) *Guidelines for Chemical Warfare Agents in Military Drinking Water.* Washington D. C. Subcommittee on Guidelines for Military Field Drinking-Water Quality, 1995.

(5) Bizzigotti, G. *Biological and Chemical Warfare Agent Dissemination*, Mitretek Systems, 2001; pp 54−58.

(6) Kukkonen, J.; Riikonen, K.; Nikmo, J.; Jappinen, A.; Nieminen, K. *J. Hazard. Mater.* **2001**, 165−179.

10.1021/ac050278f CCC: $30.25
Published on Web 06/15/2005

the agents typically responsible for blistering action.[8] Blood borne agents—such as prussic acid (AC) or cyanogen chloride (CK)—prevent tissue utilization of oxygen by inhibition of cytochrome oxidase.[9] Environment neutralization of these CWAs typically involves the degradation of the parent compound to yield various hydrolysis products.[10−12] The G-type nerve agents—which include GB, GD, and GA—rapidly hydrolyze to form various alkyl phosphonic acids.[13] V-type or VX nerve agents degrade to form alkyl phosphonic acids, phosphonothioic acids, and various alkyl aminoethanol compounds.[14] The common sulfur and arsenic containing vesicants HD and L typically degrade to produce various thiodiglycols and vinylarsonous products, respectively.[15] Blood borne agents such as AC initially hydrolyze to formamide and subsequently to ammonium formate; while CK readily hydrolyzes to hydrogen chloride and unstable cyanic acid. The cyanic acid further decomposes to carbon dioxide and ammonia.[16]

In general, CWA hydrolysis or degradation products have been found to exhibit a higher degree of stability and persistence in the environment than their corresponding parent agents.[10] Direct detection of these CWA degradation products has provided a convenient and indirect detection method for the presence or past presence of CWAs. The degradation products of CWAs are typically polar and nonvolatile in character, readily dissolving in aqueous environments. A host of stand-alone analytical techniques in an assortment of forms—liquid chromatography (LC),[17] gas chromatography (GC),[18] ion chromatography,[19] capillary zone electrophoresis,[12] mass spectrometry (MS),[20] and ion mobility spectrometry (IMS)[21]—have been employed for the analysis of these CWA degradation products with varying degrees of success. Hyphenated instrumentation on the other hand has shown to be particularly advantageous in combining the complementary strengths of the individual analytical methods mentioned above for the detection of CWAs and related degradation products. Traditionally, the use of LC−MS for "nonvolatile" CWA samples combines both dependable sample separation (via LC) and adequate detection limits with unambiguous peak detection (via MS). This technique is, however, limited temporally by the comparatively slow mode of LC separation.[22] For the analysis of "volatile" CWAs, the use of various forms of GC/MS has provided an alternative approach to complement that of the liquid hyphenated systems; however, even GC/MS types of techniques still require minutes of analysis time.[23]

Recently, the development of an atmospheric pressure ion mobility spectrometer (AP-IMS) interfaced to a orthogonal reflector time-of-flight mass spectrometer (TOFMS) has demonstrated the capability—through a variety of sample introduction and ionization modes—to rapidly (<1 min) and sensitively (<100 ppb for most compounds tested) detect, identify, and quantitate both "aqueous-" and "vapor"-phase CWA degradation and simulant products, respectively.[24,25] More importantly, with the prior development of the AP-IMS[26] with resolving powers similar to or better than that of typical HPLC separations has facilitated the AP-IMS-TOFMS or IM(tof)MS to eliminate traditional chromatographic separations all together and rely solely upon the rapid (ms time scale) separation capabilities of the high-resolution AP-IMS before mass spectrometric analysis via the TOFMS. Although rapid detection of both aqueous- and vapor-phase CWA degrada-

(7) Burgen, A. S. V.; Hobbiger, S. *Br. J. Pharmacol. Chemother*. **1951**, *6*, 593−605. Koelle, G. B.; Ballantyne, B.; Marrs, T. C. *Pharmacology and toxicology of organophosphates*; Butterworth-Heinemann, Oxford, U.K., 1992; pp 35−39. Compton, J. A. F. *Military Chemical and Biological Agents: Chemical and Toxicological Properties*; The Telford Press: Caldwell, NJ, 1987. Grob, D.; Hervey, A. M. *Am. J. Med*. **1953**, *14*, 52−63. Grob, D. *Arch. Intern. Med*. **1956**, *98*, 221−239. Grob, D.; Harvey, A. M. *J. Clin. Invest.* **1958**, *37*, 350−368.

(8) Fox, M.; Scott, D. *Mutat. Res*. **1980**, *75*, 131−168.

(9) Gosselin, R. E.; Smith, R. P.; Hodge, H. C. *Clinical toxicology of commercial products*, 5th ed.; Williams & Wilkins: Baltimore, MD, 1984. Hathaway, G. J.; Proctor, N. H.; Hughes, J. P.; Fischman, M. L. *Proctor and Hughes' chemical hazards of the workplace*, 3rd ed.; Van Nostrand Reinhold: New York, 1991.

(10) Kingery, A. F.; Allen, H. E. *Toxicol. Environ. Chem*. **1995**, *47*, 155−184.

(11) Vasil'ev, I. A.; Shvyryaev, B. V.; Liberman, B. M.; Sheluchenko, V. V.; Petrunin, V. A.; Gorskii, V. G. *Mendeleev Chem. J*. **1996**, *39* (4), 3−10. Yang, Y. C.; Bake, J. A.; Ward, J. R. *Chem. Rev*. **1992**, *92*, 1729−1743. Yang, Y. C. *Acc. Chem. Res*. **1999**, *32*, 109−115. Wagner, G. W.; Yang, Y. C. *Ind. Eng. Chem. Res.* **2002**, *41* (8), 1925−1928.

(12) Cheicante, R. L.; Stuff, J. R.; Durst, H. D. *J. Capillary Electrophor.* **1995**, *4*, 157−163.

(13) Larsson, L. *Acta Chim. Scand*. **1958**, *12*, 783−785. Gustafson, R. L.; Martell, A. E. *J. Am. Chem. Soc.* **1962**, *84*, 2309−2316. Epstein, J. *Science* **1970**, *170*, 1936−1938. Ellin, R. I.; Groff, W. A.; Kaminskis, A. *J. Environ. Sci. Health, Part B* **1981**, *B16* (6), 713−717. Desire, B.; Saint-Andre, S. *Fundam. Appl. Toxicol*. **1986**, *7* (4), 646−657. Hammond, P. S.; Forster, J. S. *J. Appl. Polym. Sci.* **1991**, *43* (10), 1925−1931.

(14) Ketelaar, J. A. A.; Gersmann, H. R.; Beck, M. M. *Nature* **1956**, *177*, 392−393. Epstein, J.; Callahan, J. J.; Bauer, V. E. *Phosphorus* **1974**, *4*, 157−163. Yang, Y. C.; Szafraniec, L. L.; Beaudry, W. T.; Bunton, C. A. *J. Org. Chem*. **1993**, *58*, 6964−6965.

(15) Bartlett, P. D.; Swain, C. G. *J. Am. Chem. Soc*. **1949**, *71*, 1406−1415. Waters, W. A.; Williams, J. H. *J. Chem. Soc*. **1950**, 18−22. Yang, Y. C.; Szfraniec, L. L.; Beaudry, W. T.; Ward, R. J. *J. Org. Chem.* **1988**, *53* (14), 3293−3297. Meylan, W. M.; Howard, P. H. *J. Pharm. Sci*. **1995**, *84* (1), 83−92.

(16) Francke, S. *Manual of Military Chemistry, Volume 1. Chemistry of Chemical Warfare Agents*; Deutscher Militärverlag: Berlin (East), 1967. Translated from German by U.S. Department of Commerce, National Bureau of Standards, Institute for Applied Technology, NTIS No. AD-849 866.

(17) Roach, M. C.; Unger, L. W.; Zare, R. N.; Reimer, L. M.; Pumpliano, J. W.; Frost, J. W. *Anal Chem*. **1987**, *59*, 1056−1059. Garfield, P. J.; Pagotto, J. G.; Miller, R. K. *J. Chromatogr*. **1989**, *475*, 261.

(18) Tornes, J. A.; Johnson, B. A. *J. Chromatogr*. **1989**, *467*, 129−138. Kientz, C. E. *J. Chromatogr*. **1998**, *814*, 1.

(19) Kingery, A. F.; Allen, H. E. *Anal. Chem*. **1994**, *66* (1), 155. Bossle, P. C.; Reutter, D. J.; Sarver, E. W. *J. Chromatogr*. **1987**, *407*, 399.

(20) Berkout, V. D.; Cotter, R. J.; Segers, D. P. *Am. Soc. Mass Spectrom*. **2001**, *12*, 641−647.

(21) Eiceman, G. A.; Karpas, Z. *Ion Mobility Spectrometry*; CRC Press: Boca Raton, FL, 1994. Asbury, R. G.; Wu, C.; Siems, W. F.; Hill, H. H. *Anal. Chim. Acta* **2000**, *404*, 273−283. Tabrizchi, M.; Khayamian, T.; Taj, N. *Rev. Sci. Instrum.* **2000**, *71*, 2321−2328.

(22) Wils, E. R. J.; Hulst, A. G. *J. Chromatogr.* **1988**, *454*, 261−272. Kostianen, R.; Bruins, A. P.; Hakkinen, V. M. A. *J. Chromatogr.* **1993**, *634*, 113−118. Borrett, V. T.; Mathews, R. J.; Colton, R.; Traeger, J. C. *Rapid Commun. Mass Spectrom.* **1996**, *10*, 114. Black, R. M.; Read, R. W. *J. Chromatogr.* **1997**, *759*, 79−92. D'Agostino, P. A.; Chenier, C. L.; Hancock, J. R. *J. Chromatogr., A* **2002**, *950*, 149−156. D'Agostino, P. A.; Hancock, J. R.; Provost, L. R. *J. Chromatogr., A* **2001**, *912*, 291−299. Read, R. W.; Black, R. M. *J. Chromatogr., A* **1999**, *862*, 169−177. D'Agostino, P. A.; Hancock, J. R.; Provost, L. R. *J. Chromatogr., A* **1999**, *840*, 289−294. Black, R. M.; Read, R. W. *J. Chromatogr., A* **1998**, *794*, 233−244.

(23) Noami, M.; Kataoka, M.; Seto, Y. *Anal. Chem*. **2002**, *74*, 4709−4715. Driskell, W. J.; Shih, M.; Needham, L. L.; Dana, B. *J. Anal. Toxicol*. **2002**, *26* 6−10. Schneider, J. F.; Boparai, A. S.; Reed, L. L. *J. Chromatogr. Sci*. **2001**, *39*, 420−424. Eckanrode, B. A. *J. Am. Soc. Mass Spectrom*. **2001**, *925*, 241−249. Brickhouse, M. D.; Creasy, W. R.; Williams, B. R.; Morrissey, K. M.; O'Connor, R. J.; Durst, H. D. *J. Chromatogr., A* **2000**, *883*, 185−198.

(24) Steiner, W. E.; Clowers, B. H.; Matz, L. M.; Siems, W. F.; Hill, H. H. *Anal. Chem.* **2002**, *74*, 4343−4352.

(25) Steiner, W. E.; Clowers, B. H.; Haigh, P. E.; Hill, H. H. *Anal. Chem.* **2003**, *75*, 6068−6076.

(26) Wu, C.; Siems, W. F.; Asbury, G. R.; Hill, H. H., Jr. *Anal. Chem.* **1998**, *70*, 4929−493. Dugourd, P. H.; Hudgins, R. R.; Clemmer, D. E.; Jarrold, M. F. *Rev. Sci. Instrum*. **1997**, *68*, 1122.

tion and simulant products have been demonstrated with IM(tof)-MS technology, aerosol-phase detection of CWA degradation and simulant products have not been investigated. Therefore, this paper explores the feasibility of using IM(tof)MS technology for the detection of a G-type CWA simulant in various diversified aerosol matrixes (i.e., water, kerosene, gasoline, and diesel) at progressively increasing AP-IMS temperatures. This rapid approach should increase qualitative capacity over that possible by either ion mobility or mass spectrometry alone and significantly decrease the potential for false positive responses.

EXPERIMENTAL SECTION

Chemicals and Solvents. The CWA simulant dimethyl methylphosphonate (DMMP) used in this study was obtained as a 97% purum standard from the Sigma Aldrich Chemical Co. (St. Louis, MO). This type of compound was used to make up analytical reference solutions to simulate Schedule 1, 2, or 3 toxic chemicals or their precursors as stated in the CWC verification and related annex.[2] Aqueous-phase stock solutions of DMMP were prepared in ESI solvent (47.5% water, 47.5% methanol, 5% acetic acid) at concentrations of 1000 ppm (1000 μg/mL). Aerosol-phase stock solutions of DMMP were prepared and filtered through a 3.0-μm filter at a concentration of 1000 ppm (1000 μg/mL) in the following: water (90% water/10% 2-propanol), kerosene (90% kerosene/10% 2-propanol), gasoline (90% gasoline/10% 2-propanol), and diesel (90% diesel/10% 2-propanol) matrixes. Further dilutions of both aqueous- and aerosol-phase stock solutions to 100 and 10 ppm (100 and 10 μg/mL), respectively, depended upon the experiment. HPLC grade solvents (water, methanol, acetic acid, 2-propanol) were purchased from J. T. Baker (Phillipsburgh, NJ). Additional aerosol matrixes (kerosene, gasoline, diesel) were purchased from Texaco fueling facilities (Pullman, WA).

Instrumentation. The IM(tof)MS instrument used in this study was constructed at Washington State University, where the fundamental components (^{63}Ni ionization source, ESI source, AP-IMS drift tube, pressure interface, TOFMS analyzer, data acquisition system) and modes of operation have been previously described in considerable detail.[24,25,27] Thus, only additional components not yet described, such as the cyclonic aerosol generator, are explained below. For quick reference, the overall IM(tof)MS operating conditions summary can be found in Table 1.

In the IM(tof)MS schematic shown in Figure 1, a Elemental Scientific (Omaha, NE) quartz PFA-ST cyclonic aerosol chamber operating at 2.59×10^3 Torr N_2 (solution flow rate of 20 μL/min) was used in conjunction with a heated (75−75 °C) stainless steel transfer line (3.0-mm outer diameter (o.d.) and 2.5-mm inner diameter (i.d.)) to introduce 1.0−5.0-μm aerosol CWA simulant samples into a stainless steel inlet ring on the AP-IMS. The stainless steel sample inlet ring was constructed such that the stainless steel transfer line carrying the neutral aerosol samples of interest were transported directly from the cyclonic aerosol generator into the reaction region of the AP-IMS tube. The stainless steel sample inlet ring was located ~4.0 cm from the front of the AP-IMS target screen.

Table 1. IM(tof)MS Operating Conditions Summary

Electrospray Ionization	
ESI voltage	1.20×10^4 V
ESI sampling rate	5.0 μL/min
sampling concentration	10 ppm
Cyclonic Aerosol Introduction	
nitrogen cyclonic aerosol pressure	2.59×10^3 Torr
aqueous sampling rate	20.0 μL/min
liquid sampling concentration	100 ppm
aerosol droplet diameter	1.0−5.0 μm
ionization source	^{63}Ni
Ion Mobility Spectrometer	
pressure	694 Torr
temperature	75, 100, 150, 200, 250, 275 °C
target screen voltage	9.00×10^3 V
gate voltage	8.14×10^3 V
drift length	18.0 cm
drift gas inlet block voltage (shower head)	156.0 V
nitrogen drift gas flow rate	1.0 L/min
Pressure Interface	
pressure	1.4 Torr
nozzle lens	150 V
focus lens	145 V
skimmer lens	92.3 V
Time-of-Flight Mass Spectrometer	
pressure	2.10×10^{-6} Torr
lens 1	−12.0 V
lens 2	−138.0 V
deflector up lens 3	−2.6 V
deflector down lens 4	−0.2 V
lens 5	0.1 V
reflector back plane	648.0 V
reflector grid plane	−243.4 V
extraction region loading	−713.0 V
extraction region pulsing	763.0 V
flight region	-2.00×10^3 V
MCP bias	1.52×10^3 V
Acquisition Timing	
TOFMS resolution	1.25 ns
IMS gate pulse frequency	25.0 Hz
IMS gate pulse width	200.0 μs
TOFMS extraction frequency	50 kHz
TOFMS extraction pulse width	2.0 μs
Miscellaneous	
all sampling	3-min runs
all sampling sets	3 runs per data point

Once in the reaction region, neutral aerosols of the CWA simulant were swept along via a countercurrent flow of preheated (75−275 °C) nitrogen drift gas toward the target screen of the AP-IMS. Here upon aerosol desolation, secondary ^{63}Ni ionization of the neutral CWA simulant vapor occurred. Ionized CWA simulants then drifted under a weak uniform electric field (443 V/cm) through the two regions (reaction (8.0 cm in length) and drift (18.0 cm in length)) of the AP-IMS tube (maintained at a temperature of 75−275 °C) toward the TOFMS. CWA simulant ions that exited the AP-IMS drift tube (694 Torr) needed to traverse a pressure interface (1.4 Torr) before they were transported through a series of lenses into the TOFMS (2.10×10^{-6} Torr) for analysis.

Acquisition of data for this experimental sequence consisted of a timing mechanism that was composed of a real-time three-dimensional (3-D) matrix of simultaneous intensity, mobility drift, and mass flight times. Ions were typically gated for 200 μs into

(27) Steiner, W. E.; Clowers, B. H.; Fuhrer, K.; Gonin, M.; Matz, L. M.; Siems, W. F.; Schultz, A. J.; Hill, H. H. *Rapid Commun. Mass Spectrom.* **2001**, *15*, 2221. Shumate, C. B.; Hill, H. H. *Anal. Chem.* **1989**, *61*, 601. St. Louis, R. H.; Hill, H. H., Jr. *Crit. Rev. Anal. Chem.* **1990**, *21*, 321−355.

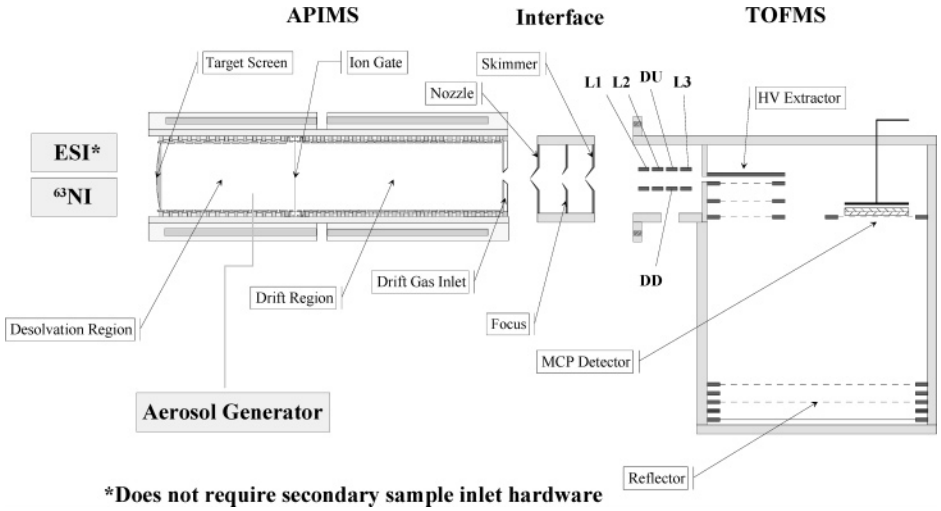

Figure 1. Schematic diagram of the IM(tof)MS instrument. Aqueous-phase samples were introduced and ionized via a standard ESI source. Aerosol-phase samples were produced with a cyclonic aerosol generator and introduced via a secondary inlet port fitted to the IM(tof)MS via a stainless steel inlet ring in the reaction region of the AP-IMS tube. Ionization of the aerosol samples was facilitated by a traditional ^{63}Ni source.

the drift region at a frequency of 25.0 Hz. This allowed for a maximum of 40 ms for the AP-IMS mobility data to be acquired. The TOFMS extraction frequency was set to 50.0 kHz, which provided a mass spectrum that consisted of ions with flight times up to 20 μs. Therefore, within each 40-ms mobility time window there were effectively 2.00×10^3 TOF extractions.

The AP-IMS ion gate, TOFMS extractor, and TOFMS time-to-digital converter were all triggered by a personal computer (PC)-based timing controller. Synchronization of this electronic hardware was facilitated by the use of a dual Pentium III workstation running Ionwerks[28] 3-D acquisition software. Experimental data acquisitions were run in triplicate for a typical run time of 3.0 min to provide adequate ion statistics. Once acquired, spectral compilations of data were then exported into Research Systems IDL virtual machine 6.0 software for processing.[29]

Calculations. For this discussion, the term drift time, t_d, of an ion in the AP-IMS drift tube is defined as the time required for ions to travel through the length of the drift cell space, L, in centimeters, as given by

$$t_d = L^2/KV \quad (1)$$

where the mobility of the ions, K (in cm^2/V·s), is inversely related to the potential drop, V (in V), they experience across the drift region. To correct for varying environmental and experimental conditions, it is practical to report ion drift times in terms of reduced mobility constants (K_o),[26] which are defined by

$$K_o = \left[\left(\frac{L^2}{Vt_d}\right)\left(\frac{273.15}{T}\right)\left(\frac{P}{760}\right)\right] \quad (2)$$

where L is the drift region length (18.0 cm), V is the drift voltage (7.98×10^3 V) or voltage drop from the AP-IMS gate to the drift gas inlet block, T is the effective temperature in the drift region (348.15−548.15° K), and P is the pressure (694 Torr).

RESULTS AND DISCUSSION

Two modes of operation were used with the IM(tof)MS instrument in this study to explore the detection of a G-type CWA simulant in diversified aerosol matrixes at progressively increasing AP-IMS temperatures: an aqueous-phase mode and a aerosol-phase mode. The aqueous-phase mode was included in this study to be used as a standard with which to compare the results obtained form the various aerosol experiments. In the aqueous-phase mode, aqueous samples were introduced and ionized directly into the IM(tof)MS by an ESI source. In the aerosol-phase mode, aerosol CWA simulant samples were introduced into the IM(tof)MS by a heated stainless steel transfer line as described above and upon desolvation ionized by a ^{63}Ni ionization source. All data obtained in this study—with corresponding ions, masses, drift times, K_o values, and arbitrary signal intensities for the CWA simulant DMMP investigated—are reported in Table 2 for each of the analysis methods employed.

Aqueous-Phase Mode. A standard aqueous-phase reference solution for the CWA simulant DMMP was prepared and electrosprayed at a rate of 5 μL/min into the IM(tof)MS instrument. The 3-D spectrum (shown centered in Figures 2 and 3) shows the 3-D separation of an acquisition (3.0 min) of a solution (10 ppm) conducted at progressively increasing AP-IMS temperatures (75−275 °C). Ions from the CWA simulant DMMP were identified as the singly protonated $(M + H)^+$ peak. These 3-D spectra allowed for the direct determination of corresponding ions, masses, drift times, K_o values, and arbitrary signal intensities produced from a standard ESI experimental aqueous-phase method to that of an aerosol-phase mode. Moreover, the comparison of these experimentally determined K_o values to some of those found in the literature, as shown in Table 2, helps to further validate the use of the IM(tof)MS instrument for the accurate identification of CWA simulants.[21]

Although the rapid detection of the CWA simulant DMMP was achieved at all temperatures in a single 3-D spectrum, further

(28) Ionwerks 3-D, Ionwerks Inc., Houston, TX, 2004.
(29) Transform V3.4, *Fortner Software LLC*; Serling VA, 1998. Research Systems IDL virtual machine 6.0, Research Systems Inc., Boulder CO, **2004**.

Table 2. Thermal Effects on the Detection of CWA Simulant DMMP in (1) an Aqueous-Phase Mode Employing Standard ESI Techniques and (2) an Aerosol-Phase Mode Which Investigated Various Sample Matrixes (Water, Kerosene, Gasoline, Diesel) with Corresponding Ions, Masses, Drift Times, K_o Values, and Arbitrary Signal Intensities.

		drift times (μs), K_o, intensity (RSD)[a]				
temp (°C)	ions $(M + N)^n$ mass (Da)	ESI[b]	water aerosol	kerosene aerosol	gasoline aerosol	diesel aerosol
75	$(M + H)^+$/125	2.180×10^4 **1.33** 93.0 (3.8)	2.166×10^4 **1.34** 126.0 (3.15)	2.168×10^4 **1.34** 103.0 (3.74)	2.177×10^4 **1.33** 110.0 (3.36)	2.185×10^4 **1.33** 100.0 (3.60)
100	$(M + H)^+$/125	2.028×10^4 **1.34** 157.0 (3.58)	2.019×10^4 **1.34** 172.0 (2.81)	2.019×10^4 **1.34** 173.0 (4.90)	2.019×10^4 **1.34** 163.0 (5.34)	2.019×10^4 **1.34** 165.0 (3.44)
150	$(M + H)^+$/125	1.798×10^4 **1.33** 724.0 (3.45)	1.796×10^4 **1.33** 759.0 (3.83)	1.796×10^4 **1.33** 723.0 (4.54)	1.798×10^4 **1.33** 766.0 (3.93)	1.798×10^4 **1.33** 717.0 (4.61)
200	$(M + H)^+$/125	1.617×10^4 **1.32** (1.32, 1.30) 1.24×10^3 (4.27)	1.623×10^4 **1.32** 1.45×10^3 (3.74)	1.628×10^4 **1.31** 1.33×10^3 (4.13)	1.626×10^4 **1.32** 1.27×10^3 (5.12)	1.627×10^4 **1.32** 1.26×10^3 (3.24)
250	$(M + H)^+$/125	1.494×10^4 **1.30** 1.48×10^3 (4.65)	1.491×10^4 **1.30** 1.55×10^3(2.93)	1.489×10^4 **1.30** 1.58×10^3 (3.56)	1.491×10^4 **1.30** 1.57×10^3 (3.68)	1.489×10^4 **1.30** 1.52×10^3 (3.89)
275	$(M + H)^+$/125	1.405×10^4 **1.32** 1.39×10^3 (3.78)	1.416×10^4 **1.31** 1.47×10^3 (4.32)	1.413×10^4 **1.31** 1.42×10^3 (2.97)	1.413×10^4 **1.31** 1.66×10^3 (3.65)	1.416×10^4 **1.31** 1.52×10^3 (4.04)

[a] Values, in descending order, for each temperature: arbitrary signal intensity; percent relative standard deviation (RSD) for three experimental runs. [b] ESI literature K_o values.[25]

examination of Figures 2 and 3 showed that not only was the singly protonated $(M + H)^+$ peak present but some were considerably more intense. Analysis of both the AP-IMS mobility and TOFMS spectrums for these peaks showed that, for a given temperature, an arbitrary signal intensity could be assigned to be more or less prominent in intensity depending upon AP-IMS temperature. For example, at a temperature of 75 °C as shown in Figure 2, a mobility drift time of 2.180×10^4 μs, the 125.0-Da DMMP ion was observed to be clearly resolved from the baseline noise with a arbitrary signal intensity of 93.0. Conversely, Figure 3 at 275 °C shows the mobility drift time shortened to 1.405×10^4 μs for the 125.0-Da DMMP ion, but the arbitrary signal intensity was found to increase to 1.39×10^3. This dramatic increase in signal intensity of 1.30×10^3 is thought to be attributed to the ability of the reaction region of the AP-IMS to desolvate the CWA simulant DMMP analyte for ionization.[25]

Aerosol-Phase Mode. In these experiments, aerosol-phase samples were produced via a quartz cyclonic chamber and introduced—via a heated stainless steel transfer line—into the IM-(tof)MS between the ionization region and the AP-IMS ion gate, as shown in Figure 1. The ionization source used to ionize the neutral vapors produced from the aerosol-phase CWA simulant in the IM(tof)MS were based on secondary gas-phase chemical ionization[21] via a traditional ^{63}Ni ionization source commonly used with IMS technology. Figures 2 and 3 show acquisitions (3.0 min) of a 100 ppm mixture of DMMP in water, kerosene, gasoline, and diesel matrixes conducted at progressively increasing AP-IMS temperatures (75−275 °C). These 2-D IM(tof)MS spectrums are accompanied by a combination of both the extracted mobility (shown on the side of the 2-D spectrum) and the mass (shown above the 2-D spectrum) spectra. Ions from the CWA simulant DMMP were identified as the singly protonated $(M + H)^+$ peak in all four matrixes, where the overall extracted mobility/mass IM(tof)MS data from the 2-D data matrix were acquired at once. This made it possible to clearly determine the arbitrary signal intensities, mobility drift times, and ion masses for each of the ions produced, thus allowing for the rapid direct comparison between these values with all four types—water, kerosene, gasoline, and diesel—of solution matrixes.

When determining the applicability of using IM(tof)MS technology to monitor the presence of CWA simulant DMMP in aerosol-phase samples, it was found that the ions produced from the secondary ^{63}Ni ionization were the same regardless of what sample matrixes (i.e., water, kerosene, gasoline, or diesel) or AP-IMS temperatures (75−275 °C) were employed. Yet even more interesting was that both mobility drift times and ion masses matched the values shown in Table 2 for standard ESI of the aqueous-phase samples shown above. An example of this can be seen in Figure 3 where the mobility/mass of 1.405×10^4 μs/125.0 Da for the standard ESI of the aqueous-phase solution and the mobility/mass of 1.416×10^4, 1.413×10^4, 1.413×10^4, and 1.416×10^4/125.0 Da for the water, kerosene, gasoline, and diesel aerosol-phase samples were within 95% confidence with respect to one another in mobility and exact in mass, respectively. The significance of this was seen as dramatic; IM(tof)MS has now shown the accuracy, precision, and robustness to sample in both the aqueous-phase and complex aerosol-phase matrixes, yielding corroborating mobility/mass values with little to no competing sample interferences. Additionally, even though the detection of the CWA simulant DMMP was achieved in a single IM(tof)MS spectrum four all four matrixes, it was still essential not to overlook the importance of the combined 3-D spectrum mode of the IM-(tof)MS analysis and the additional identification power it provides for the rapid identification of these agents.

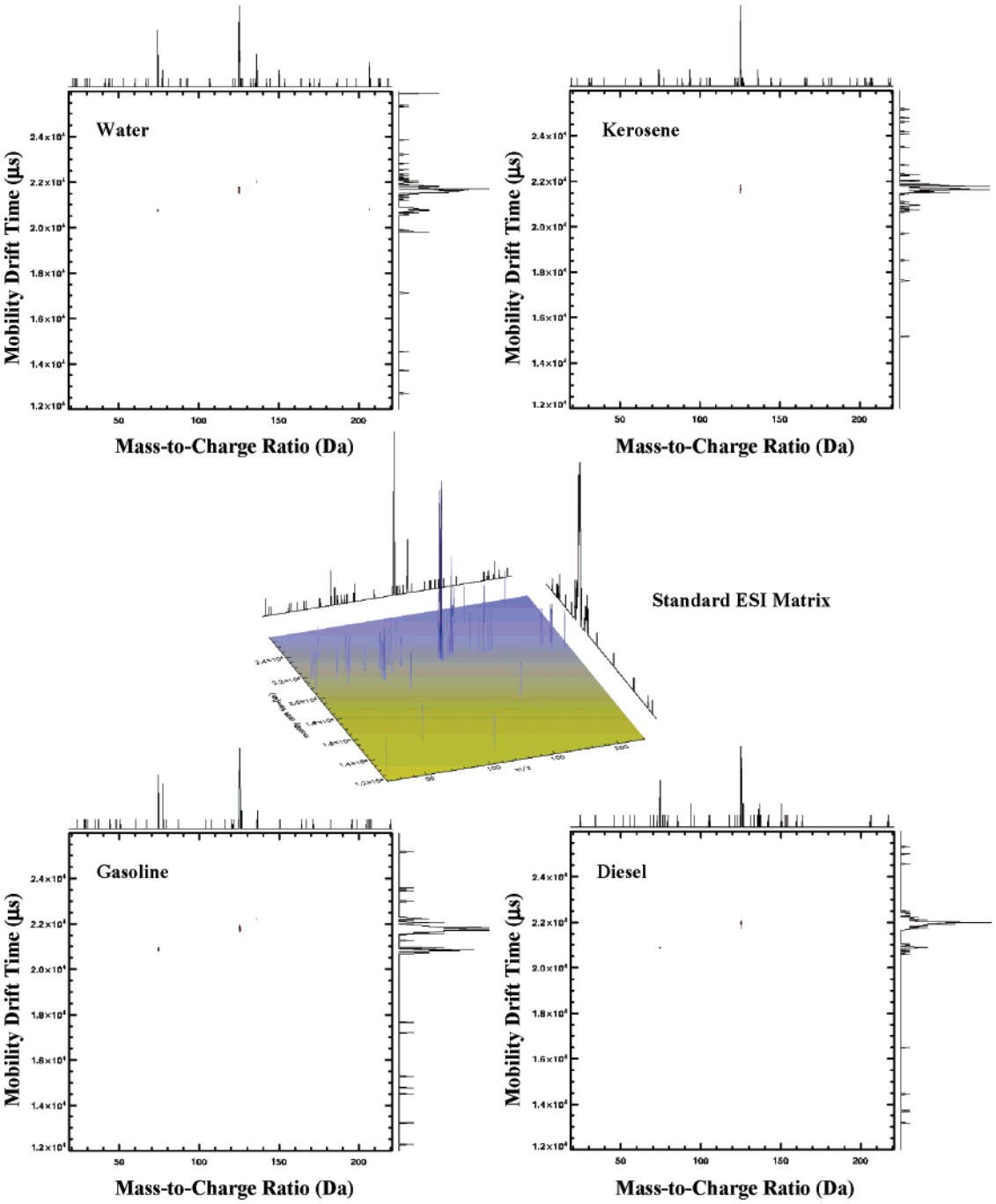

Figure 2. Secondary ^{63}Ni ionization (at 75 °C) of a 100 ppm aerosol-phase mixture of the CWA simulant DMMP by both the 2-D mobility mass spectrum and extracted mobility mass spectra in water, kerosene, gasoline, and diesel matrixes. The ESI of a 10 ppm aqueous-phase mixture containing the CWA simulant DMMP is also shown as the centered 3-D spectrum of mobility drift times and mass-to-charge ratios. Ions from the CWA simulant DMMP were identified as the single $(M + H)^+$ peak.

Last, the arbitrary signal intensities of the singly protonated $(M + H)^+$ CWA simulant DMMP ion fluctuated depending upon what AP-IMS temperature (75−275 °C) was employed, but not with respect to each matrix for that given temperature. For example, at a temperature of 75 °C as shown in Figure 2, the arbitrary signal intensities of the DMMP ion in water, kerosene, gasoline, and diesel were 126.0, 103.0, 110.0, and 100.0, respectively. These data yielded an average arbitrary signal intensity (109.8 ± 11.6) with a 10.1 coefficient of variation for the four sample matrixes. Whereas, in Figure 3, the arbitrary signal intensities of the DMMP ion in water, kerosene, gasoline, and diesel were found to increase to 1.47×10^3, 1.42×10^3, 1.66×10^3, and 1.52×10^3, respectively; yielding an average arbitrary signal intensity of $1.52 \times 10^3 \pm 103.4$ with a 89.5 coefficient of variation for the four sample matrixes at 275 °C. Comparison of the average arbitrary signal intensities for 75 °C to that of 275 °C shows that there was at least 1 order of magnitude difference in arbitrary signal intensity observed. This dramatic increase in signal intensity—as seen above with the employment of an ESI source operating in the aqueous-phase mode—was also thought to be attributed to the ability of the reaction region of the AP-IMS to desolvate a potential analyte for ionization. Again it is important

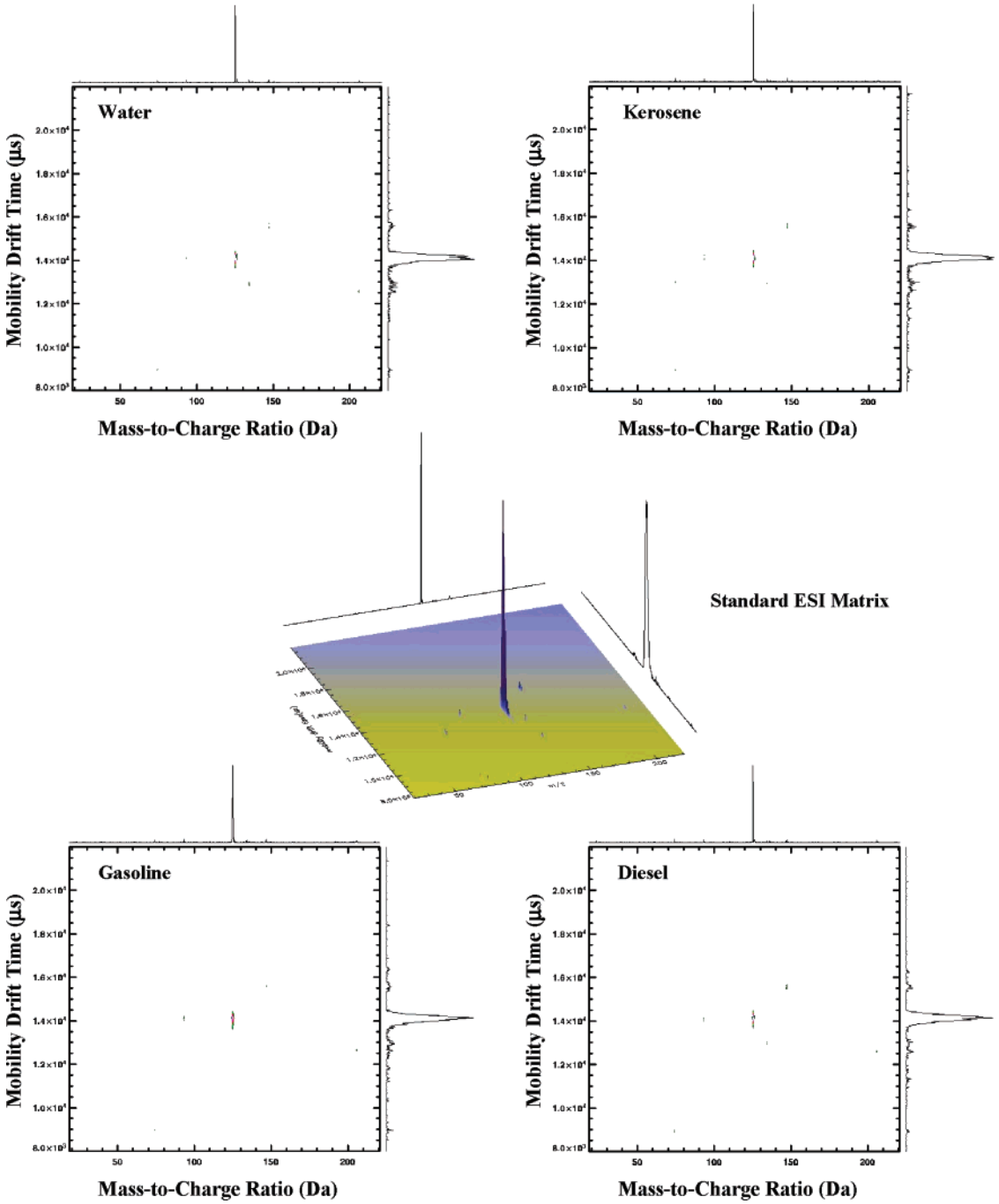

Figure 3. Secondary ^{63}Ni ionization (at 275 °C) of a 100 ppm aerosol-phase mixture of the CWA simulant DMMP by both the 2-D mobility mass spectrum and extracted mobility mass spectra in water, kerosene, gasoline, and diesel matrixes. The ESI of a 10 ppm aqueous-phase mixture containing the CWA simulant DMMP is also shown as the centered 3-D spectrum of mobility drift times and mass-to-charge ratios. Ions from the CWA simulant DMMP were identified as the single $(M + H)^+$ peak.

to note that all experimental conditions (i.e., temperature, pressure, voltage, etc.) were exactly the same for each aerosol matrix employed. Moreover, the reference CWA simulant DMMP solutions were run in triplicate and repeated on three separate occasions producing repeatability values within a 95% confidence level experimentally.

CONCLUSIONS

The main advantage of IM(tof)MS over IMS or MS technology is its ability to provide both a 3-D and a 2-D data acquisition spectrum with the capacity to electronically couple and decouple collision-induced dissociation to generate ion fragmentation patterns to facilitate the identification of mobility selected ions, permitting compound identification and significantly reducing the number of false positive responses.[25] Here the employment of IM(tof)MS has now shown the capacity (accuracy, precision, robustness) to be used for the G-type DMMP CWA aerosol-phase sample in a variety of sample matrixes (water, kerosene, gasoline, diesel) at progressively increasing AP-IMS temperatures (75−275 °C) with little to no competing sample interferences. As the AP-IMS

temperature was increased from 75 to 275 °C there was seen an order of magnitude increase in arbitrary signal intensity for the CWA simulant DMMP ion, regardless of which sample matrixes were employed. Additionally, both mobility drift times and ion masses were found to match one another regardless of what sampling mode was employed (i.e., aqueous or aerosol). The significance of this allows IM(tof)MS technology to sample in either the aqueous phase or aerosol phase while still retaining the ability to yield corroborating mobility/mass values. While these studies were limited to the detection of a single G-type CWA simulant in a variety of aerosol matrixes and temperatures, the analytical principles demonstrated in this study are expected to be applicable to a wide range of compounds in diversified matrixes.

ACKNOWLEDGMENT

The authors acknowledge the Edgewood Chemical Biological Center, Aberdeen Proving Grounds, MD, for their continued scientific correspondence. This work was supported in part by Geo-Centers Incorporated (Grants 40853CMGC3173 and 42090SM).

Received for review February 15, 2005. Accepted May 13, 2005.

AC050278F